Microwave-driven plasma gasification for biomass waste treatment at miniature scale

Sturm, Guido S J; Navarrete Muñoz, Alex; Purushothaman Vellayani, A.; Stefanidis, Georgios D.

DOI
10.1109/TPS.2016.2533363

Publication date
2016

Document Version
Accepted author manuscript

Published in
IEEE Transactions on Plasma Science

DOI: 10.1109/TPS.2016.2533363

Microwave-driven plasma gasification for biomass waste treatment at miniature scale

Guido S.J. Sturm[a], Alexander Navarrete Muñoz[a,b], P.V. Aravind[a], Georgios D. Stefanidis[c,*]

[a]Process and Energy Department, Delft University of Technology, Leeghwaterstraat 39, 2628 CB Delft, The Netherlands

[b]Department of Chemical Engineering and Environmental Technology, University of Valladolid, c/Doctor Mergelina s/n, 47011 Valladolid, Spain

[c]Chemical Engineering Department, Katholieke Universiteit Leuven, Celestijnenlaan 200f, 3001 Leuven, Belgium

* Corresponding author (georgios.stefanidis@cit.kuleuven.be)

Abstract

Gasification technology may combine waste treatment with energy generation. Conventional gasification processes are bulky and inflexible. By using an external energy source, in the form of microwave-generated plasma, equipment size may be reduced and flexibility as regards the feed composition may be increased. This type of gasification may be combined with fuel cell technology to generate electricity for on-site microwave generation. In this work, we present short gasification experiments with cellulose, as model biomass compound, in air plasma. In order to optimize reaction rates, gasification and plasma generation are combined in the same volume in order to expose the solids to plasma of maximum intensity. The heating value of the fuel gas yield exceeds, up to 84%, the net microwave energy transmitted into the reactor over a range of operating conditions. As the system has not been optimized, in particular regarding residence time, the results give confidence that this concept can eventually be developed into a viable small-scale decentralized gasification technology.

Keywords

Microwave plasma, plasma gasification, biomass, cellulose, waste

1. Introduction

In view of the scarcity of energy resources, concern about emissions, and the growing population, two future challenges can be identified. These are the effective exploitation of renewable energy sources, and destruction and/or utilization of organic waste materials. The conversion process that is typically considered for such challenge is gasification, which is a process converting organic feedstock into fuel gas, and which has already been widely demonstrated at large scale.

For those situations, however, in which no or very little supporting infrastructure is available, or for cases that require relatively small and mobile installations, no satisfactory solutions do yet exist. This holds for the context of this present study that is supported by the Bill & Melinda Gates Foundation in the context of the "Reinvent the Toilet Challenge" [1]. This challenge aims to provide global sanitation improvement by providing of small and mobile treatment units for human waste materials in developing regions. The requirements also hold for many other conceivable situations that require small scale waste destruction, such as for example local destruction of chemical waste or shipborne waste destruction.

Another potential area of application that is gaining attention is small-scale conversion and storage of energy for load leveling of renewable power generation. The IEA Technology Roadmap Energy Storage reports a need for a 310 GW storage capacity to accommodate a 27-44% renewable electricity production in 2050; it also reports that the technologies considered in this context – flywheel technologies, supercapacitors, superconducting magnetic energy storage, battery technology, pumped storage hydropower, and compressed air energy storage – are challenged in terms of high costs, large footprint, and low energy density [2]. Another technology discussed in this context by both the IEA report and Turner [3] are water electrolyzers, hydrogen storage, and fuel cells; as with the other technologies, though, it is pointed out that costs remain a challenge in the foreseeable future. An alternative may be found by enhancing the aforementioned gasification process with renewable energy, thereby storing this energy in the fuel gas that is produced. The specific method of enhancement considered in the context of this study is combining gasification with plasma. A notable aspect of plasma is that in principle it can respond fast to intermittent and fluctuating energy demand and supply. Downscaling will remain an important consideration for this kind of application, though. Typically, process systems loose dynamic responsiveness as they get larger, so exploring the downscaling limitations will remain worthwhile.

Gasification is a process in which solid feedstocks such as biomass and coal are made to react with a gasification agent such as air, steam or oxygen under sub-stoichiometric conditions resulting in the formation of syngas, i.e. a mixture of hydrogen and carbon monoxide, which is an easy to handle gaseous fuel and which forms a building block for production of storable fuel and chemicals. Conventionally, gasification is carried out using different reactor types such as fixed bed gasifiers, fluidized bed gasifiers or entrained flow gasifiers [4]. However, theses reactor types are used in general to process easily gasified feedstocks such as clean wood, low ash content coal etc. While small scale gasification is achieved using fixed bed reactors for example in cooking applications [5,6], well prepared wood chips or pellets are in general required for ensuring smooth operation of the reactors. Furthermore, conventional gasification requires part of the feedstock to be combusted to provide the process with sufficient thermal energy. The syngas produced can be used for several purposes, it can serve as a raw material for chemicals manufacture, but in the context of this study its utilization in energy generation, conversion and storage is considered. At large scale conventional syngas based thermal power production systems are in principle feasible [7], but at small power levels these are inefficient. It has been shown that SOFCs can operate at small power levels (few kW) with very high efficiency [8]. System studies have also indicated that, biosyngas, once cleaned, can be fed to small-scale SOFCs or SOFC integrated systems so as to produce electric power at high efficiencies [9,10]. Further studies have been conducted into the influence of biomass derived contaminants on SOFCs [11,12], gas cleaning systems have been developed [12] and successful gasifier-SOFC integrated operation has been achieved [13]. Present research efforts aim to keep extending the operational flexibility of the gasification process in terms of size and feedstock.

Plasma enhanced gasification

The introduction of thermal plasma into the gasification process may be the key towards process downscaling and enhancing flexibility. The external energy source – the electromagnetic field that energizes the plasma – provides an additional degree of freedom to the process that enables process adaption to feedstock variations in terms of both feeding rate and composition. In case of plasma, the external energy source originates in electrical power, possibly from renewable sources. This avoids the requirement to provide energy to the process by means of partial combustion of the feedstock. In principle, dilution of product gasses with combustion products can thus be avoided; in addition, renewable energy can be stored as heating value of the product gasses. Further, plasma enables intense conditions 4000–5000 K in case of a microwave plasma and even higher at 10000–12000 K in case of

an ICP or arc discharge plasma [14]. The intensity allows for rapid processing, lower residence time required, and thus a volumetric process scale-down or miniaturization; furthermore, the intensity enables utilization of feedstocks that are resilient to thermal processing, such as municipal solid waste [15], and do not readily break down in conventional gasifiers. In addition, plasma has been shown to facilitate the reforming – and thereby destruction – of tar that is commonly formed in gasification and that is generally considered problematic [16]. Finally, the additional energy source provides a means to compensate for heat losses that become more constricting as the size of conventional – non-plasma – gasification systems is reduced. Naturally, heat losses compromise efficiency, but below a certain geometrical size threshold – as they become more dominant in the overall energy balance – they might also inhibit conventional gasification processes, because the process will no longer be able to sustain its operational temperature.

At large scale, the technical feasibility of plasma gasification is demonstrated by Willis et al. [17]. The authors reported on the design and operation of a large (104 MW fuel gas output) plasma-assisted gasification plant for waste materials. It concerns a system that uses high power (3.22 MWe) arc-plasmas, and thus it demonstrates the general technological and operational feasibility of plasma-assisted waste gasification. Further, a theoretical framework is being developed with several researchers publishing regularly on the subject [18–20]. Other relevant experimental work at smaller scale has been published by Moustakas et al. [21], Lemmens et al. [22], Hong at al. [23], and Uhm et al. [24]. The latter two publications are relevant in the context of this present research since in they report on operation of and gasification with a 915 MHz microwave generated plasma. The latter publication reports on brown coal gasification by microwave-generated steam plasma; a reasonably high cold gas efficiency of 84 % is reported for a medium size gasification unit (500 kW fuel gas output). A number of these authors were also involved in studies on smaller scale 2.45 GHz microwave plasma gasification of brown coal [25] and coal [26] with 8 kW of fuel gas output, and – due to scaling laws – a lower cold gas efficiency at 43 %. Further work at the same scale was done by Yoon and Lee [27, 28], which saw successful gasification of coal and charcoal.

In a collaborative effort on the development of the aforementioned project on processing of human waste materials, Liu at al. [29] present a system integration study of a small-scale ~10 kW fuel gas output plasma gasifier integrated with a solid oxide fuel cell (SOFC) stack, a pre-treatment stage for drying and grinding, and a gas cleaning stage to prepare the syngas for the SOFC. It is shown by means of simulation that such a combined system for decentralized treatment of human waste may

indeed form an energetically self-sustained process, which would enable the objective of developing a small-scale processing facility for sanitation waste that is non-reliant on pre-existing infrastructures (i.e. water supply, sewage, electricity supply, and fuels). The feasibility of fuel cell integration was also explored by another group, Galvita et al. [30], and shown to have potential. The purpose of this present study is to focus on the plasma gasification step in the context of the above collaborative effort to develop the larger treatment and energy recovery system.

The specific requirements of the intended application pose several tough challenges: the system has to be small, so that heat losses are relatively large and efficiency is limited; the infrastructure limitations do not leave much freedom in terms of plasma agent, as only air is essentially available; and only technologies that in principle are robust and can be manufactured at low cost can be considered.

It is not known what the limits are to which the plasma gasification process can be downscaled while retaining adequate effectiveness, but in order to achieve the highest processing rate we expose the feedstock to the plasma at its spatially highest intensity. Specifically, we combine the gasification process and plasma generation in the same part of the reactor, so that gasification occurs in plasma at its maximum intensity.

In order to meet the robustness and cost requirements we use a microwave field, which is preferred over an arc discharge plasma or an inductively coupled plasma, because magnetron vacuum tubes are more cost-effective and fit the power required by our application better than the alternatives, while still providing a reliable means to generate an electromagnetic field. In addition, in contrast to arc discharge plasma, microwave generated plasma avoids direct contact of the plasma with electrodes, so electrode wear is avoided.

At present, the interplay between the physical phenomena occurring in the plasma gasification reactor thus specified is not known, and design strategies for developing such reactors do not yet exist. Hence we start our exploration with off-the-shelf parts in order to verify the feasibility of the process. Similar to Konno et al. [31] we use cellulose as a model substance for waste materials.

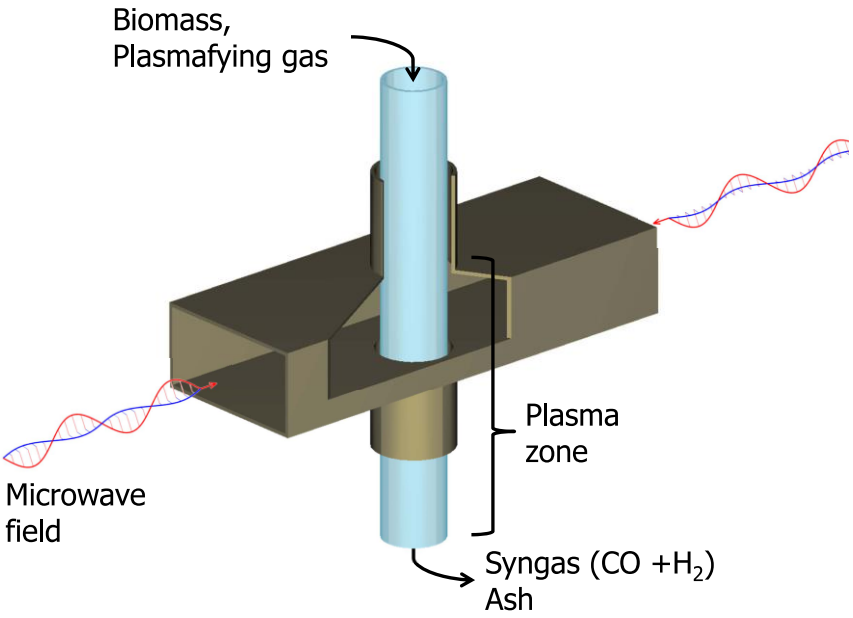

Figure 1. Schematic of the plasma gasification reactor assembly.

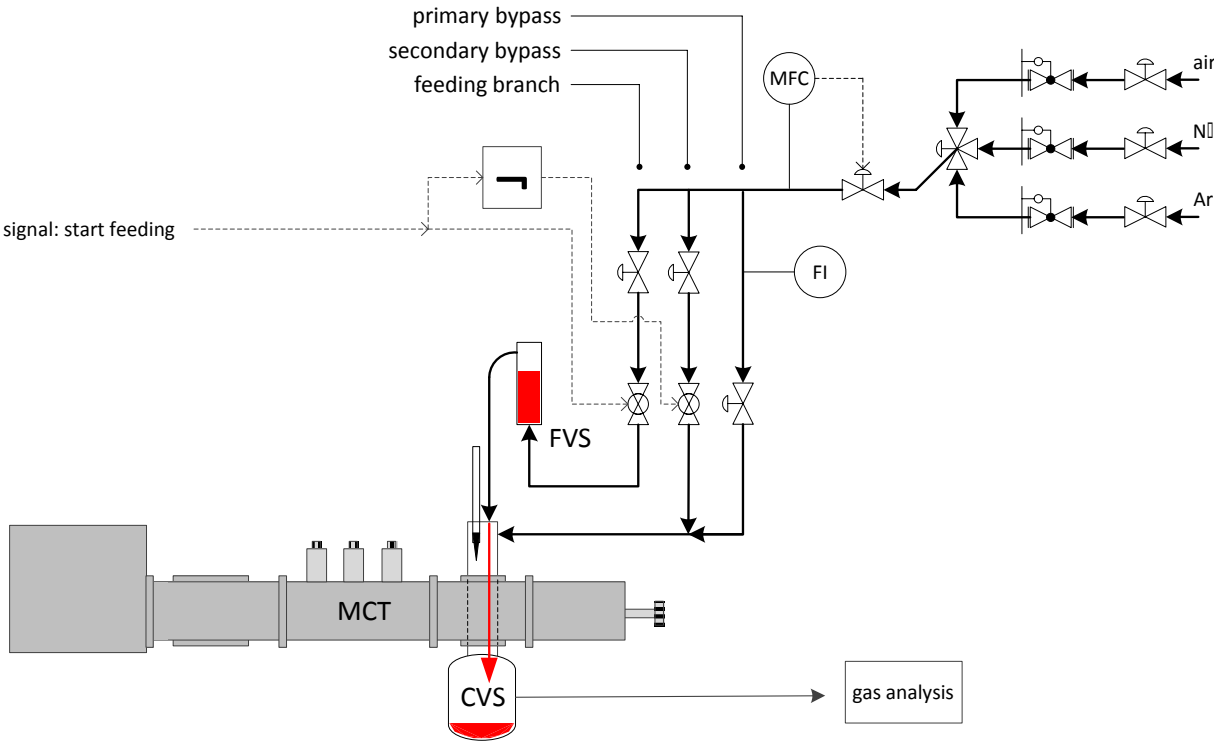

Figure 2. Schematic of the experimental system. MCT: microwave circuit; FVS: feeding vessel; CVS collection vessel; MFC: mass flow controller; FI: flow indicator.

2. Experimental apparatus and methodology

The gasification reactor is essentially constructed out of a quartz pipe with an internal diameter of 31 mm and a wall thickness of 2 mm that crosses the broad face of a WR-340 waveguide. Figure 1 presents a schematic of the assembly; the quartz pipe is oriented vertically and the waveguide is placed along the horizontal plane. Metal pipes run along the quartz pipe both from the top and the bottom onto the waveguide wall. These pipes are dimensionalized with an internal diameter that is narrow enough to block microwave transmission at the wavelength that the system operates at; thus, the microwave field is contained in the waveguide, while gas and solids are free to flow through the quartz pipe. Further relevant dimensions of the reactor assembly are listed as follows: the cavity formed by waveguide is at the location of the reactor 71 mm high; the section of the reactor passing through a metallic cut-off pipe directly downstream of the cavity is 100 mm long; this is followed by roughly 60 mm leading into the collection vessel (CVS, see below). The assembly of plasma generator and reactor are based on, and modified from the commercially available *Downstream Plasma Source* obtained from Sairem SAS [32]. Due to the high temperatures involved (4000-5000 K, [14]) and the presence of a strong microwave field, in situ temperature measurement is not possible in the reactor. The quartz pipe containing the hot plasma is contacted on the outside by air and the waveguide parts at room temperature; a thermal balance between heating and cooling is maintained, so that melting of the pipe is avoided. It did require a significant effort of testing and repairing before suitable operating conditions were found.

The reactor operated at ambient pressure; i.e. its outlet is at ambient pressure and due to the flow rates and piping diameters involved, only negligible pressure drop occurs in the system. In the context of this study air is fed from the top into the quartz reactor pipe both as a plasma agent and oxidizer. Before plasma ignition, an ignition electrode system is lowered into the quartz pipe down to the level of the waveguide. Once microwave field generation starts, an initial discharge on the electrode absorbs electromagnetic energy from this field. This discharge then grows into a plasma flame that is blown downwards with the gas stream. After ignition, the electrode is retracted from the reactor and plasma is sustained as long as the microwave field is present.

Once plasma has been ignited, solid biomass is also fed from the top into the quartz pipe. As it passes through the plasma flame, the high temperatures and reactive plasma species cause the biomass to

gasify, which results in the production of fuel gas in the form of hydrogen, carbon monoxide and methane.

Figure 2 presents a schematic of the experimental system. The microwave part of the system is an electromagnetic circuit in typical layout [33] that is constructed out of several WR-340 waveguide elements. The microwave system operates at a frequency of 2.45 GHz, which is compatible with the WR-340 waveguide standard. This frequency was chosen due to the relative compactness of the waveguide elements. The reactor assembly is an integral part of this microwave circuit (MCT) that in all consists of the following parts:

- A 2.45 GHz microwave generator with a maximum output power of 6 kW.
- An isolator, which is a microwave circuit element that protects the microwave generator from exposure to a reflected microwave field. More specifically, it transmits a microwave field traveling in the forward direction, but absorbs it when it travels in the reverse direction.
- An impedance transformer, which is a circuit element that can be used to tune the microwave field in the circuit such that no reflections occur towards the generator. Essentially, proper tuning causes the energy of the microwave field to be largely dissipated by energizing the plasma, thus enabling good utilization efficiency of the microwave energy.
- The reactor assembly, as described above.
- A variable reflector that can be used to position the standing microwave field in the microwave circuit. Tuning of this element allows the positioning of a microwave field maximum at the plasma flame, facilitating energy transfer from the microwave field to the plasma.

All microwave circuit parts were obtained from Sairem SAS [32]. This includes the waveguide parts of the reactor assembly, which were later modified to better suit our needs. Figure 3 shows a photograph of the setup layout.

The flow system is configured as follows:

- Gas enters the system through a mass flow controller (MFC, Bronkhorst F-201AV-50K) with which the total gas flow is regulated.
- After the MFC, the flow is split into three branch lines. Each branch includes a needle valve that enables adjustment of the flow rate through it. One branch line flows to the feeding vessel (FVS, discussed below) while the two other branches bypass the feeding vessel and flow directly into the reactor.
- Of the bypass branch lines, the primary one includes a flow indicator (FI). Both the secondary bypass line and the branch line that flows to the feeding vessel include an automatic valve. These automatic valves are controlled such that if one opens, the other one closes. The needle valves in the separate branch lines are balanced such that the total flow rate through the MFC is not affected once the automatic valves switch the gas flow from one branch line to the other. The flow indicator can be used to verify this.
- Initially, the feeding vessel is loaded with solid biomass powder and the branch line to the feeding vessel is closed so no gas flows through the feeding vessel. The secondary bypass line is opened. Once a signal is generated to start feeding, the branch line to the feeding vessel opens and the secondary bypass line closes. The gas flow enters the feeding vessel in the bottom side; the upward flow through the powder bed fluidizes this bed and gradually carries the entrained particle bed into the reactor.
- After the particles pass the plasma zone in the reactor, the remains are captured in a collection vessel (CVS). The gas flow exits the reactor and passes a sample point before being disposed in ventilation. The sample point has a multi-way valve with three ports to mount gas sample bags on.

In all, the experimental procedure is as follows:

- Preparatory experiments are conducted to adjust the needle valves to the desired settings, i.e. they are set such that 1) the total flow rate is little affected by switching from the secondary bypass line to the feeding vessel line, and 2) the desired solids flow rate is achieved once this switch has occurred.
- The feeding vessel is loaded with a weighed amount of powdered solid biomass. The gas line to the feeding vessel is closed and the secondary bypass line is opened.

- The total flow rate is set with the MFC; a set point value for microwave generation is given to the microwave generator though microwave generation does not start at this point.
- The ignition electrode is lowered to the level of the microwave zone. Then, microwave generation is started and after plasma ignition, the ignition electrode is retracted.
- Forward and reflected power are automatically monitored and logged. Once the plasma ignition signature in these signals is detected by the control system, solids feeding starts automatically after a timed interval by switching gas flow from the secondary bypass line to the feeding vessel line.
- After the experiment, the remaining solid biomass powder in the feeding vessel is collected and weighed. Dividing the mass difference – the mass fed to the reactor – by the total process time yields the feeding rate of the solids.
- The gas samples collected in the bags are analyzed by gas chromatography (Varian CP4900).

All automated procedures were implemented in a LabView 2010 [34] environment.

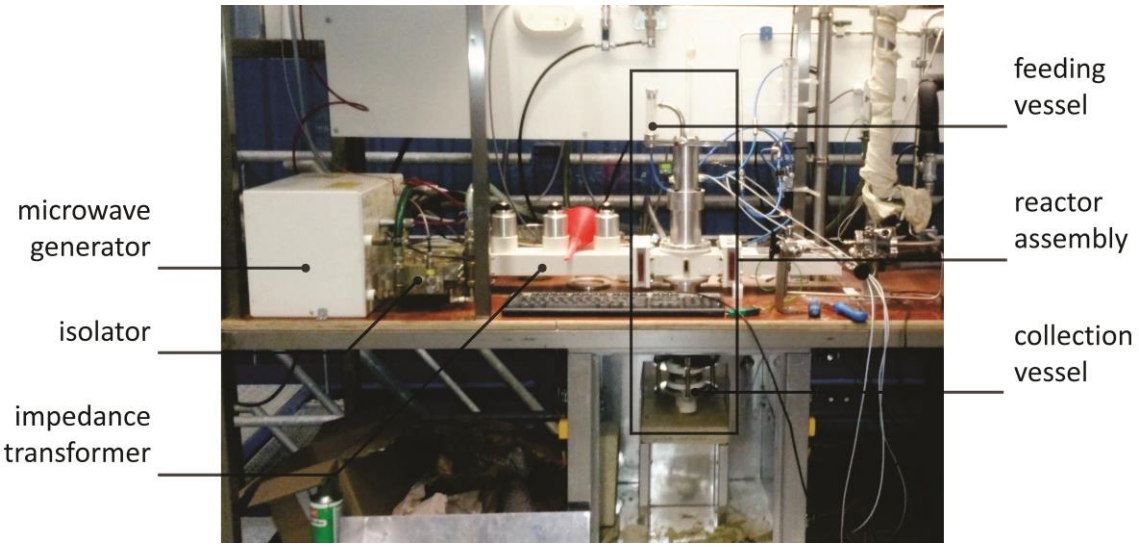

Figure 3. Photograph of setup with main parts indicated.

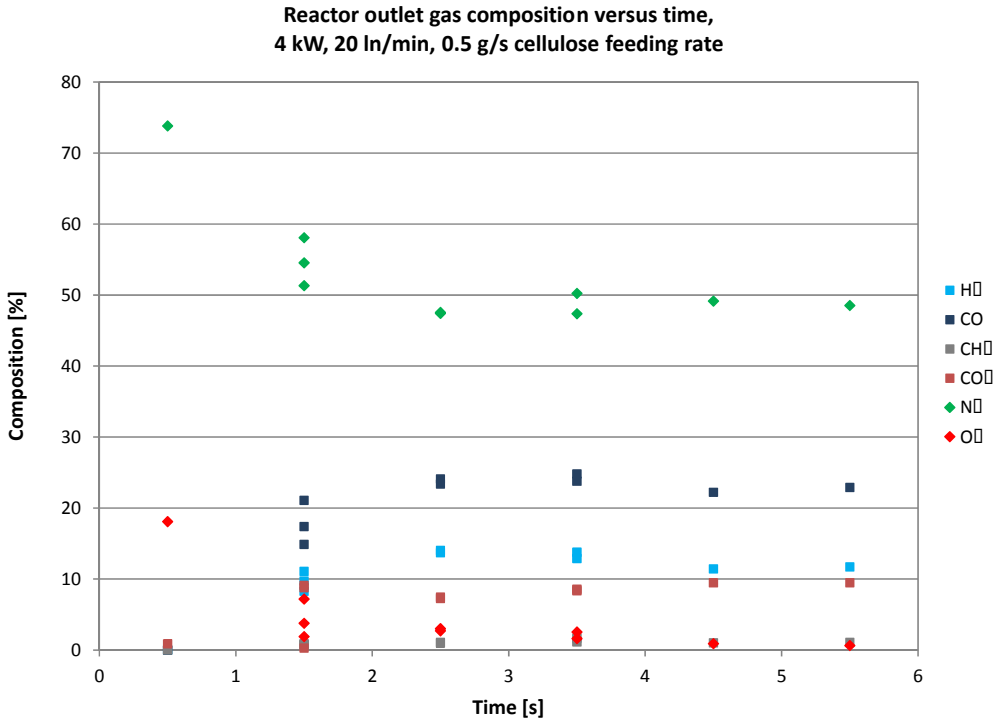

Figure 4. Transient product gas composition (mol%).

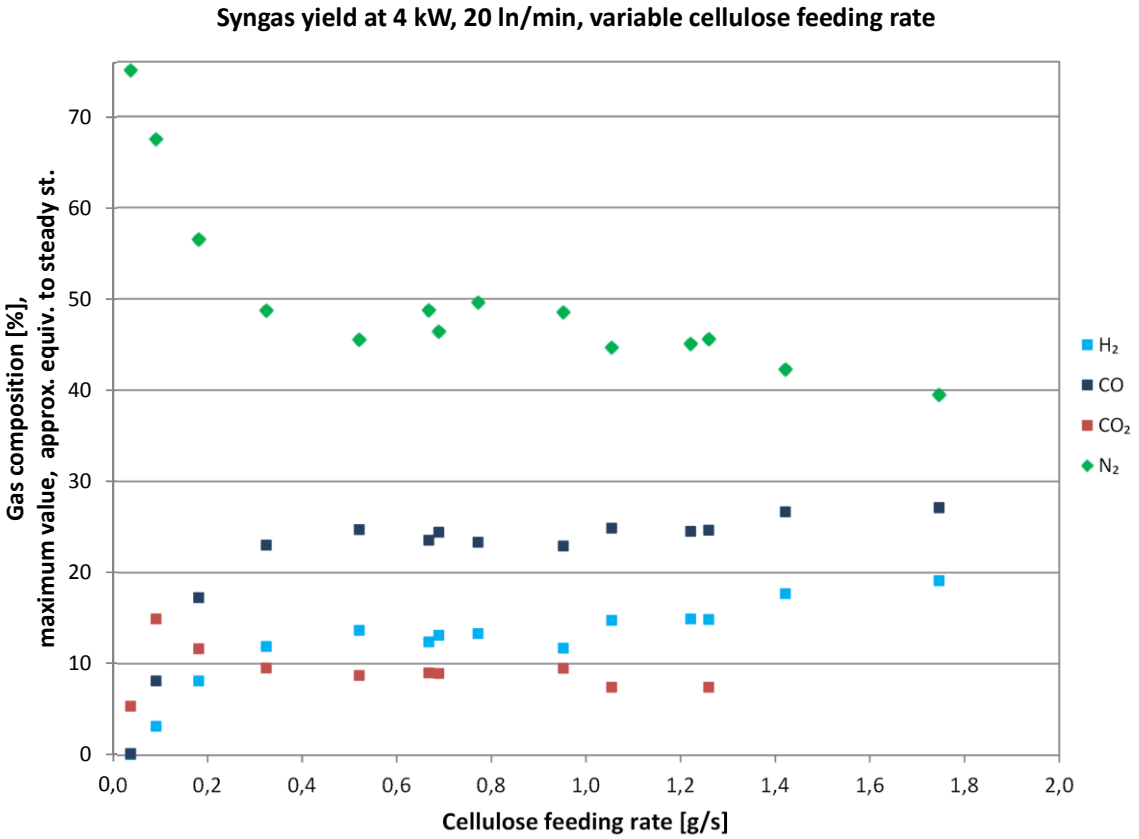

256

257 Figure 5. Quasi-steady state fuel gas composition (mol%) at the reactor outlet vs. cellulose feeding rate.

258

The experiments were conducted with air as a plasma agent and cellulose ($(C_6H_{10}O_5)_n$, obtained from Aldrich, microcrystalline, 10-350 μm measured with Microtrac S3500) as a model biomass compound. During preparatory experimentation it was found that the process appeared to perform best around the following parameter settings: a feeding rate of air of 20 natural liters (i.e. at 0 °C and 1 atm) per minute (ln/min); a forward microwave power of 4 kW; and a cellulose feeding rate of 0.5 grams per second; this amounts to an air to fuel equivalence ratio of 0.17. These conditions were the starting point for a subsequent parametric study. Repeated experiments were conducted with the same process parameters in terms of microwave power, air feeding rate and cellulose feeding rate, but with varied timing of 1 sec gas sampling intervals so as to obtain transient process data. Figure 4 presents the transient reactor outlet gas composition, i.e. the gas compositions of the samples versus the respective time intervals.

In order to approximate steady state continuous operation, it is assumed that the peak concentration of fuel gas in the gas composition would correspond to the steady state value. For the graph in Figure 4, this would correspond to a yield of 14 mol% H_2 and 25 mol% CO and 1.5 mol% CH_4 at a microwave power of 4 kW, an air feeding rate of 20 ln/min and a cellulose feeding rate of 0.5 g/s. The flow rate of producer gas at the outlet is calculated by multiplying the inlet air flow rate with the ratio of the (inert) nitrogen concentration at the inlet to its concentration at the outlet; in Figure 4 this outlet flow rate would correspond to 32 ln/min. By varying the cellulose feeding rate, the relation of gas composition versus cellulose feeding rate is obtained and shown in Figure 5; here the cellulose feeding rate varies from 0.05 to 1.75 g/s, while air feeding rate and microwave power remain constant at 20 ln/min and 4 kW.

3. Results and discussion

From the aforementioned plots, a number of process characteristics can be derived. A general feature, notable in both Figure 4 and 5, is the relatively clear trends that the data points form. This indicates that for these particular experimental conditions, the process is reproducible and stable. In addition, the process is dynamically fast, which is apparent from the graphs of the gas composition transients in Figure 4, as they reach the maximum fuel gas yield in only a few seconds. Further, methane concentration is relatively low (~1.5 mol%). Finally, as mentioned above, the yield of producer gas is roughly 30 ln/min.

The most notable feature in the trend of the fuel gas concentration versus cellulose feeding rate (Figure 5) is the initial fast rise followed by stagnation for cellulose feeding rates beyond 0.5 g/s. It appears that this plateau-like trend in the fuel gas yield occurs because of the short residence time that is estimated at 20 to 50 ms. More specifically, as the solids feeding rate increases, the fuel gas production may rise, but this will also increase the gas volume and flow velocity. This would reduce the residence time and the process effectiveness. It is further noted here that raising the microwave power does not improve performance; although more power would increase temperature and thus the rate of heat and mass transfer and reaction rates, gas expansion would also accelerate the flow, again cutting short the residence time.

The incomplete conversion is also apparent from the cellulose collected in the collection vessel. As cellulose contains no inorganics, full conversion into gas is possible provided sufficient contact time with plasma. In contrast though, the material collected in the collection vessel still resembles cellulose, albeit with a light yellow/brown hue suggesting light tar deposition. Due to the nature of the experimental procedure, a precise mass balance over the reactor could not be established. In particular, transient effects hinder calculation of an accurate figure based on the carbon balance between the cellulose that was fed and the outlet gas yield; moreover, the mass balance over the feeding vessel and collection vessel is considered imprecise, because part of the solids may have been carried further downstream by the gas flow. Nevertheless, from the available experimental data presented in Figure 5, an estimate for the conversion was made based on the carbon balance. It was found that at a cellulose feeding rate of 0.5 g/s, approx. 45 % of the cellulose mass is converted into fuel gas, which corresponds to 0.24 g/s in absolute terms. Further, at 1.7 g/s feeding rate the conversion has dropped to 15 %, corresponding to 0.26 g/s conversion rate. Overall, between the 0.5 and 1.7 g/s feeding rates, the conversion rate appears steady between 0.21 and 0.26 g/s and in agreement with the plateau-like trend described above. The exact cause of the limited conversion cannot be stated conclusively. Because of the specific interactions between plasma flame, microwave field, and gas flow patterns, the plasma does not distribute evenly over the cross-section of the quartz tube, which could mean that cellulose partially bypasses the plasma flame. However, heat and mass flow limitations between the plasma and the individual cellulose particles might also occur due to the short contact time (20-50 ms) and the low density of plasma.

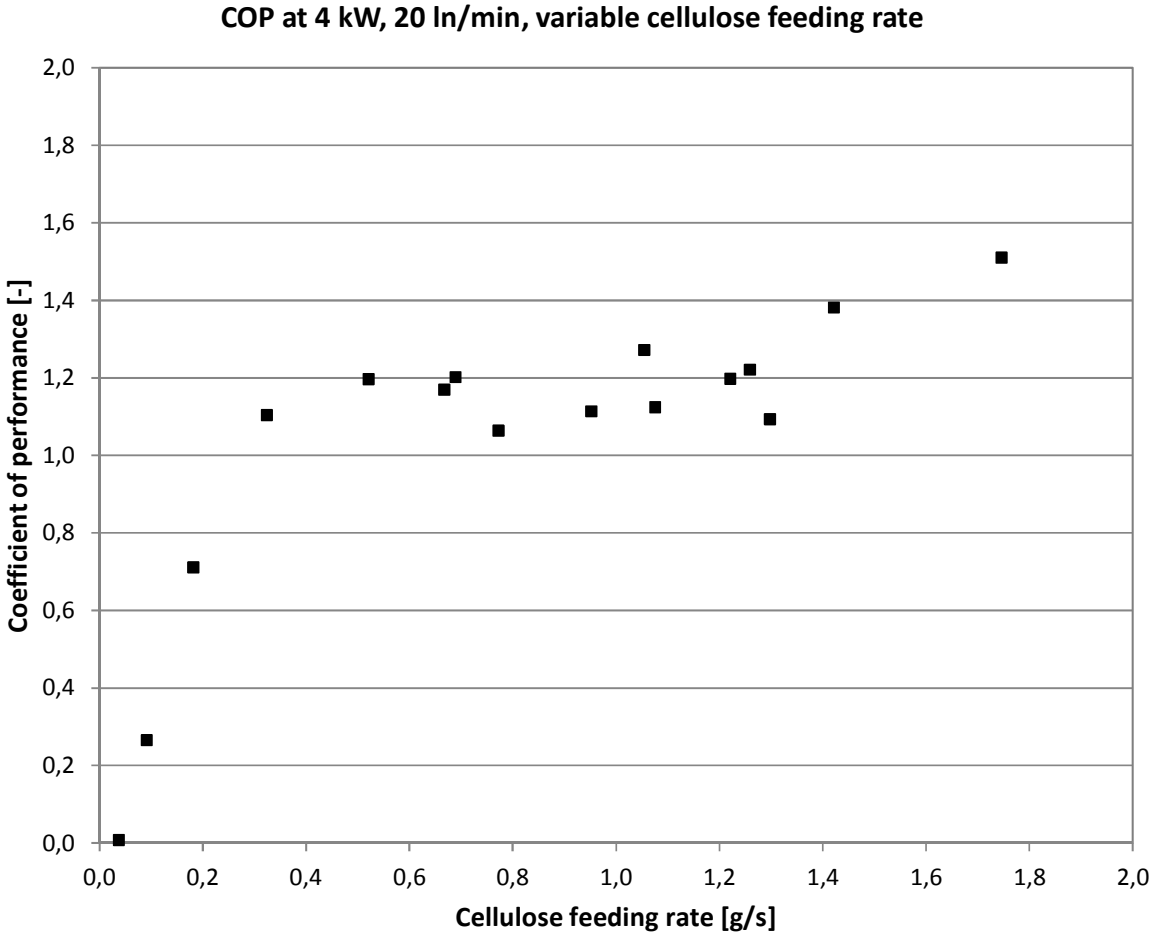

318

319 Figure 6. Coefficient of performance versus cellulose feeding rate at forward microwave power of 4 kW and air
320 feeding rate of 20 ln/min.

321

Enhancing the residence time by increasing the process volume would appear to be a straightforward way to improve conversion and, ultimately, waste destruction. The reactor presented in this study is a modified commercial off-the-shelf device that is not optimized for this gasification process. As a first design iteration, it demonstrates the feasibility of plasma gasification at this scale, though it is decidedly non-optimal. Subsequent design iterations will improve performance further, for example by applying an electromagnetic field with a longer wavelength or combining multiple plasma generators in series in the gasification system.

Despite the issues related to conversion and residence time, the chemical energy produced by the process gives a promising outlook in the context of the intended application – small- or miniature-gasification for decentralized waste treatment. Figure 6 presents the coefficient of performance of the gasification process for the experimental conditions and outlet gas compositions in Figure 5. In this context, this coefficient is defined as the ratio of the chemical energy contained in the produced fuel gas versus the net microwave transmission as described by the following formula:

$$\text{coefficient of performance} = \frac{\frac{Q_{in}}{V_m}\frac{x_{N_2,air}}{x_{N_2,out}}\left(x_{H_2,out}\Delta H_{LHV,H_2} + x_{CO,out}\Delta H_{LHV,CO} + x_{CH_4,out}\Delta H_{LHV,CH_4}\right)}{P_F - P_R} \quad (1)$$

Here Q_{in} is the volumetric flow rate of air into the reactor; V_m is the gaseous molar volume; $x_{N2,air}$ is the mole fraction of nitrogen in air; $x_{N_2,out}$, $x_{H_2,out}$, $x_{CO,out}$ and $x_{CH_4,out}$ are the mole fractions in the reactor outlet stream of N_2, H_2, CO and CH_4 respectively; $\Delta H_{LHV,H_2}$, $\Delta H_{LHV,CO}$ and $\Delta H_{LHV,CH_4}$ are the molar lower heating values of H_2, CO and CH_4 respectively [35]; P_F is the forward microwave power and P_R is the reflected microwave power. The molar fuel gas output is calculated relative to the nitrogen flow; the fuel gas flows are then multiplied with the respective lower heating values; the sum of these products is then divided by the difference of the forward microwave power and the reflected microwave power. This is the aforementioned ratio of chemical energy in the fuel gas versus net microwave transmission towards the plasma reactor. Table 1 presents the values of the parameters in Eq. 1 for the outlet gas compositions in Figure 5 at a solids feeding rate of 0.52 g/s.

Table 1. Parameters in the calculation of the coefficient of performance, for the gas composition presented in Figure 5 at a solids feeding rate of 0.52 g/s.

Q_{in}	20	ln/min
	0.33	l/s (0 °C, 1 atm)
V_m	22.41	l/mol (0 °C, 1 atm)
$x_{N_2,air}$	78.08	%
$x_{N_2,out}$	45.52	%
$x_{H_2,out}$	13.65	%
$x_{CO,out}$	24.7	%
$x_{CH_4,out}$	1.15	%
$\Delta H_{LHV,H_2}$	240.8	kJ/mol [35]
$\Delta H_{LHV,CO}$	282.6	kJ/mol [35]
$\Delta H_{LHV,CH_4}$	801.8	kJ/mol [35]
P_F	4	kW
P_R	1.61	kW
COP	1.19	-

It can be seen in Figure 6 that the coefficient of performance exceeds unity for cellulose feeding rates greater than ~0.3 g/s, while it fluctuates around 1.2 for feeding rates between ~0.3 and ~1.5 g/s. Beyond 1.5 g/s, the coefficient appears to be rising further to ~1.5. These results are promising because although the process is non-optimized, there already is a surplus of energy. We expect that process improvement, most notably on the residence time aspect, will enable better conversion, higher release of fuel gas, and enhanced energy surplus. The methods noted above could be a starting point towards this objective. Further, improved management of radiative heat losses could be applied to improve process performance.

The process was further investigated by varying the microwave power and air flow rate parameters in relation to the base case described above. The procedures above were repeated with A) the microwave power reduced to 3 kW and the same flow rate of 20 ln/min, B) proportional reduction in both parameters (i.e., microwave power of 3 kW and flow rate of 15 ln/min) and C) reduction in only the flow rate to 15 ln/min, while retaining a 4 kW microwave power. The resulting graphs of gas composition vs. cellulose feeding rate are presented in Figures 7a to c, respectively.

The graphs at reduced power (3 kW, Figures 7a-b) show similar trends as Figure 5, with the one in Figure 7a being slightly lower. This indicates that the processes are comparable. One major difference is in the stability of the plasma flame. In the cases of Figures 7a and 7b, the plasma would quench, i.e., the lower intensity microwave field would not sustain it, much more often than in the case presented in Figure 5. This instability is also apparent from the fact that the highest cellulose flow rate at which plasma could be sustained in Figures 7a-b is ~0.7 g/s, while in Figure 5, it is ~1.8 g/s. A mechanism that may be at play here is that the endothermicity of the process cools down the plasma, which reduces the electron density and electrical conductivity of plasma. Consequently, less microwave energy would be absorbed, resulting in progressive reduction of temperature up to the point where ionization no longer takes place and plasma generation stops.

In Figure 7c, this type of instability is also present – no plasma can be sustained beyond roughly 0.87 g/s –, though another type of instability is much more apparent. In Figures 5 and 7a-b, the trends formed by the data points are fairly clear, whereas in Figure 7c, a much larger spread in the gas composition can be observed. Strikingly, within this set of experiments, at the same experimental conditions, the best yield of 35 % CO and 24 % H_2 is contrasted to the worst yield of 17 % CO and 10 % H_2. The latter experiment being an actual attempt to repeat the former with the same settings in terms of microwave power, air flow rate and valve settings. The feeding rate of cellulose in both cases is around 0.4 g/s, though not exactly the same due to the limitations of the solids feeding method employed.

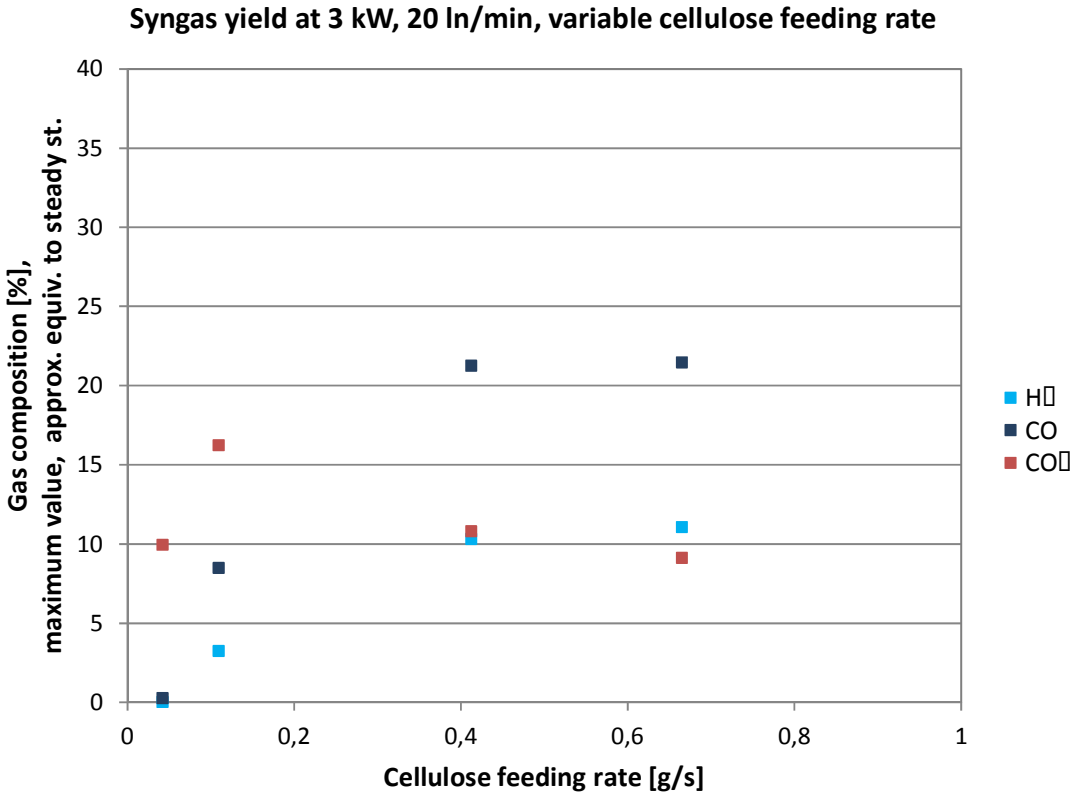
Syngas yield at 3 kW, 20 ln/min, variable cellulose feeding rate
Gas composition [%], maximum value, approx. equiv. to steady st.
Cellulose feeding rate [g/s]
0
5
10
15
20
25
30
35
40
0
0,2
0,4
0,6
0,8
1
H
CO
CO

383 (a)

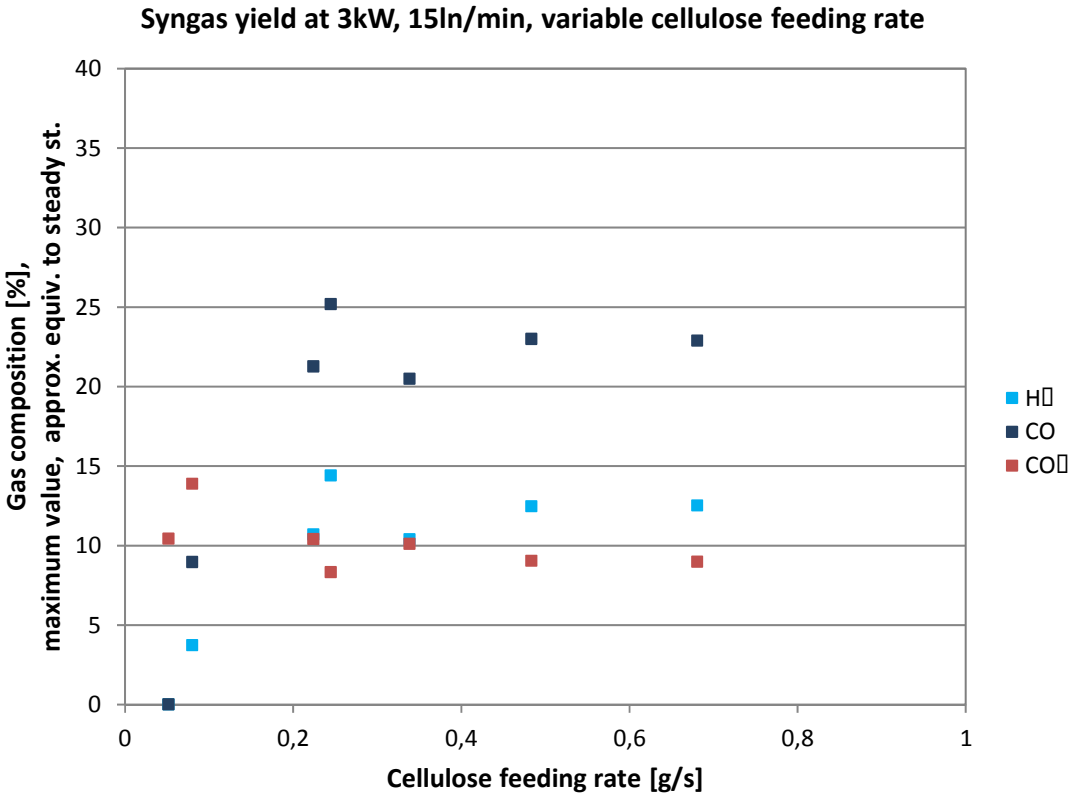
Syngas yield at 3kW, 15ln/min, variable cellulose feeding rate
Gas composition [%], maximum value, approx. equiv. to steady st.
Cellulose feeding rate [g/s]
0
5
10
15
20
25
30
35
40
0
0,2
0,4
0,6
0,8
1
H
CO
CO

384 (b)

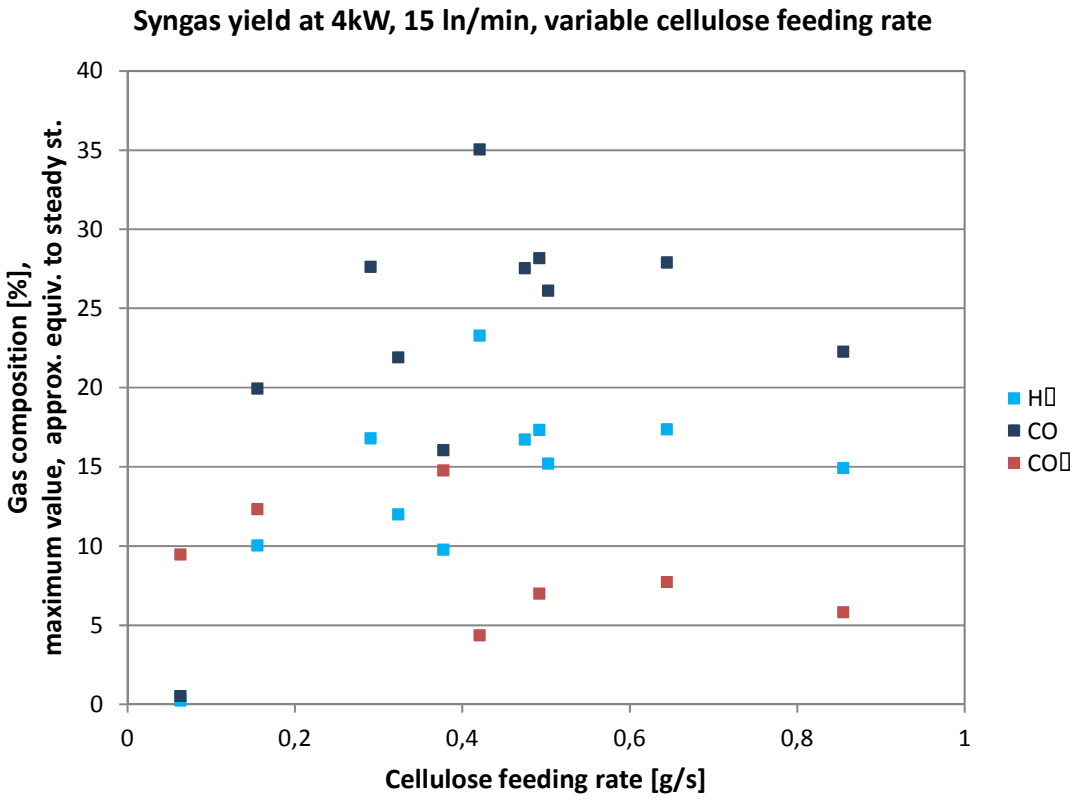

(c)

Figure 7. Quasi-steady state fuel gas composition (mol%) at the reactor outlet at vs. cellulose feeding rate under variation of forward microwave power and air flow rate: a) 3 kW and 20 ln/min; b) 3 kW and 15 ln/min; c) 4 kW and 15 ln/min.

Table 2. Maximum coefficient of performance from the data in Figures 5 and 7a-c in the 0-1 g/s cellulose feeding rate interval.

Microwave power	Air flow rate	Coefficient of performance
3 kW	15 ln/min	1.19
3 kW	20 ln/min	1.30
4 kW	15 ln/min	1.84
4 kW	20 ln/min	1.20

Table 2 presents the maximum coefficients of performance in the 0 to 1 g/s interval of the cellulose feeding rate for the variations in microwave power and gas flow rate presented in this work (Figures 5, 7a-c). For the cases of 4 kW and 20 ln/min; 3 kW and 20 ln/min; and 3 kW and 15 ln/min, the coefficients of performance are comparable at ~1.2–1.3. For the case of 4 kW and 15 ln/min, the maximum coefficient of performance is 1.84; i.e. *84% more energy* is contained in the heating value of the fuel gas obtained than was applied by the net microwave energy input. Despite this being a single case, it does further strengthen the confidence that the gasification process may attain an energy recovery sufficiently high to allow for energetically self-sufficient integration with a gas cleaning/fuel cell system downstream. The instabilities and fluctuations observed also point out the need to gain an intricate understanding of the complex interrelating phenomena that occur in this gasification process. Design and optimization of this reactor requires insight into the microwave field/plasma interactions, the dynamics of gaseous and powder flow, the heat transfer and chemical conversions, as well as into the manner in which these aspects interrelate.

4. Conclusions

In this study we evaluate a 2.45 GHz microwave plasma system for single pass gasification of solid biomass. The application context for this system is small-scale waste destruction, energy recovery, and renewable energy storage in the form of chemicals. We combine gasification and plasma generation in a single volume to maximize process intensity and speed, and to minimize equipment size. This nature of the work is exploratory to investigate process feasibility. Since it uses a modified off-the-shelf plasma generator, not a design optimized for this process, there is room to improve performance. Notably, it was found that the residence time in the system is too short for full biomass conversion. Design approaches to improve this have been suggested. We found that plasma stability poses a

challenge. Under some conditions, the plasma has a high likelihood of quenching, while under other conditions the fuel gas output and coefficient of performance are fluctuating strongly. A thorough understanding of the interrelating physical phenomena in the system will be needed for successful design and optimization of this process. Despite the challenges encountered, the process creates a surplus in energy. More specifically, the chemical energy present in the fuel gas in the outlet gas stream is up to 1.84 times higher than the energy supplied in the form of microwave energy to the gasifier, i.e. a surplus in heating value of up to 84 % is generated with respect to the microwave energy provided. These results give confidence that combining this system with a fuel cell could indeed enable energy recovery, either to form a self-sustained process, or for energy storage and recovery for load leveling purposes in renewable energy production.

Acknowledgements

We gratefully thank the Bill and Melinda Gates Foundation (contract OPP1037469) for continuous financial support of the plasma gasification research. We also thank the DEMO team at the P&E department, Verborg Engineering B.V., Euroglass Instruments B.V. (presently Trace Elemental Instruments B.V.), and J.A.S. van Driel for their active technical assistance.

References

1. Bill & Melinda Gates Foundation, *Water, Sanitation & Hygene: Reinvent the Toilet Challenge*, Bill & Melinda Gates Foundation 2013.
2. International Energy Agency, *Technology Roadmap Energy Storage*, OECD/IEA 2014.
3. J.A. Turner, A Realizable Renewable Energy Future, *Science* 285, 687–689, 1999.
4. M. Worley and J. Yale, *Biomass Gasification Technology Assessment*, Denver, NREL 2012.
5. T.B. Reed, R. Larson, A wood-gas stove for developing countries, *Energy for Sustainable Development* 3(2), 34–37, 1996.
6. S. Varunkumar, N.K.S. Rajan and H.S. Mukunda, Experimental and computational studies on a gasifier based stove, *Energy Convers. Manage.* 53, 135–141, 2012.
7. E.J.O. Promes, T. Woudstra, L. Schoenmakers, V. Oldenbroek, A. Thallam Thattai and P.V. Aravind, Thermodynamic evaluation and experimental validation of 253MW Integrated Coal Gasification Combined Cycle power plant in Buggenum, Netherlands, *Appl. Energ.* 155, 181–194, 2015.
8. M. Powell, K. Meinhardt, V. Sprenkle , L. Chick and G. McVay, Demonstration of a highly efficient solid oxide fuel cell power system using adiabatic steam reforming and anode gas recirculation, *J. Power Sources* 205, 377–384, 2012.
9. K.D. Panopoulos, L. Fryda, J. Karl, S. Poulou and E. Kakaras, High temperature solid oxide fuel cell integrated with novel allothermal biomass gasification Part II: Exergy analysis, *J. Power Sources* 159, 586–594, 2006.
10. S. Karellas, J. Karl and E. Kakaras, An innovative biomass gasification process and its coupling with microturbine and fuel cell systems, *Energy* 33, 284–291, 2008.
11. E. Lorente, M. Millan and N.P. Brandon, Use of gasification syngas in SOFC: Impact of real tar on anode materials, *Int. J. Hydrogen Energ.* 37, 7271–7278, 2012.
12. P.V. Aravind and W. de Jong, Evaluation of high temperature gas cleaning options for biomass gasification product gas for Solid Oxide Fuel Cells, *Prog. Energ. Combust.* 38(6), 737–764, 2012.
13. Ph. Hofmann, K.D. Panopoulos, L.E. Fryda, A. Schweiger, J.P. Ouweltjes and J. Karl, Integrating biomass gasification with solid oxide fuel cells: Effect of real product gas tars, fluctuations and particulates on Ni-GDC anode, *Int. J. Hydrogen Energ.* 33, 2834–2844, 2008.
14. A. Fridman and L.A. Kennedy, *Plasma Physics and Engineering* 2nd ed., Boca Raton, CRC Press 2011.
15. B. Nicolae, Plasma gasification – The waste-to-energy solution for the future, *Problemele Energeticii Regionale* 3(26), 107–115, 2014.
16. R. Monteiro Eliott, M.F.M. Nogueira, A.S. Silva Sobrinho, B.A.P. Couto, H.S. Maciel and P.T. Lacava, Tar Reforming under a Microwave Plasma Torch, *Energ. Fuel.* 27, 1174–1181, 2013.
17. K.P. Willis, S. Osada and K.L. Willerton, Plasma Gasification: Lessons learned at Ecovally WTE facility, *Proceedings of the 18th Annual North American Waste-to-Energy Conference NAWTEC18*, 2010.
18. I.B. Matveev and S.I. Serbin, Modeling of the Coal Gasification Processes in a Hybrid Plasma Torch, *IEEE T. Plasma Sci.* 35(6), 1639–1647, 2007.
19. I.B. Matveev, S.I. Serbin and N.V. Washchilenko, Sewage Sludge-to-Power, *IEEE T. Plasma Sci.* 42(12), 3876–3880, 2014.
20. R. Mourao, R. Ribeiro Marquesi, A.V. Gorbunov, G. Petraconi Filho, A.A. Halinouski and C. Otani, Thermochemical Assessment of Gasification Process Efficiency of Biofuels Industry Waste with Different Plasma Oxidants, *IEEE T. Plasma Sci.* 43(10), 3760–3767, 2015.
21. K. Moustakas, D. Fatta, S. Malamis, K. Haralambous and M. Loizidou, Demonstration plasma gasification/vitrification system for effective hazardous waste treatment, *J. Hazard. Mater.* B123, 120–126, 2005.
22. B. Lemmens, H. Elslander, I. Vanderreydt, K. Peys, L. Diels, M. Oosterlinck and M. Joos, Assessment of plasma gasification of high caloric waste streams, *Waste Manage.* 27, 1562–1569, 2007.
23. Y.C. Hong, D.H. Shin, S.J. Lee, Y.J. Kim, B.J. Lee and H.S. Uhm, Generation of High-Power Torch Plasma by a 915-MHz Microwave System, *IEEE T. Plasma Sci.* 39, 1958–1962, 2011.
24. H.S. Uhm, Y.H. Na, Y.C. Hong, D.H. Shin and C.H. Cho, Production of hydrogen-rich synthetic gas from low-grade coals by microwave steam-plasmas, *Int. J. Hydrogen Energ.* 39(10), 4251–4355, 2014.
25. Y.C. Hong, S.J. Lee, D.H. Shin, Y.J. Kim, B.J. Lee, S.Y. Cho and H.S. Chang, Syngas production from gasification of brown coal in a microwave torch plasma, *Energy* 47, 36–40, 2012.
26. D.H. Shin, Y.C. Hong, S.J. Lee, Y.J. Kim, C.H. Cho, S.H. Ma, S.M. Chun, B.J. Lee and H.S Uhm, A pure steam microwave plasma torch: Gasification of powdered coal in the plasma, *Surf. Coat. Tech.* 228, S520–S523, 2013.
27. S.J. Yoon and J.G. Lee, Syngas Production from Coal through Microwave Plasma Gasification: Influence of Oxygen, Steam, and Coal Particle Size, *Energ. Fuel.* 26, 524–529, 2012.

493 28. S.J. Yoon and J.G. Lee, Hydrogen-rich syngas production through coal and charcoal gasification using
494 microwave steam and air plasma torch, *Int. J. Hydrogen Energ.* 37, 17093–17100, 2012.
495 29. M. Liu, T. Woudstra, E.J.O. Promes, S.Y.G. Restrepo and P.V. Aravind, System development and self-
496 sustainability analysis for upgrading human waste to power, *Energy* 68 377–384, 2014.
497 30. V. Galvita, V.E. Messerle and A.B. Ustimenko, Hydrogen production by coal plasma gasification for
498 fuel cell technology, *Int. J. Hydrogen Energ.* 32, 3899–3906, 2007.
499 31. K. Konno, H. Onodera, K. Murata, K. Onoe and T. Yamaguchi, Comparison of Cellulose
500 Decomposition by Microwave Plasma and Radio Frequency Plasma, *Green Sustainable Chem.* 1, 85–
501 91, 2011.
502 32. Sairem SAS, *Les sources plasma*, 2015, available at http://www.sairem.fr/les-sources-plasma-56.html,
503 accessed 30/10/2015, and *Générateurs, composants et mesure*, 2015, available at
504 http://www.sairem.fr/generateurs-composants-et-mesure-42.html, accessed 30/10/2015.
505 33. G.S.J. Sturm A.Q. Van Braam Houckgeest, M.D. Verweij, T. Van Gerven, A.I. Stankiewicz and G.D.
506 Stefanidis, Exploration of rectangular waveguides as a basis for microwave enhanced continuous flow
507 chemistries, *Chem. Eng. Sci.* 89 196–205, 2013.
508 34. LabVIEW 2010®, Austin TX: National Instruments Corp., 2010.
509 35. The Engineering Toolbox, *Gross and Net Heating Values for some common Gasses*,
510 http://www.engineeringtoolbox.com/gross-net-heating-values-d_420.html, accessed 09/04/2015.

511